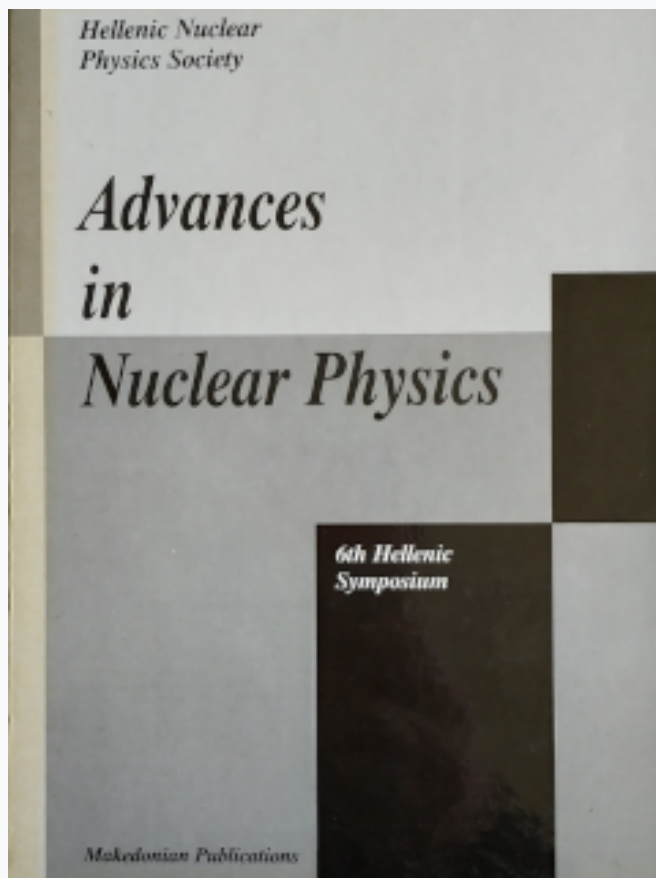


HNPS Advances in Nuclear Physics

Vol 6 (1995)

HNPS1995



Energy Structure and Distribution of Macroscopical Fermion Matter

C. Syros

doi: [10.12681/hnps.2915](https://doi.org/10.12681/hnps.2915)

To cite this article:

Syros, C. (2020). Energy Structure and Distribution of Macroscopical Fermion Matter. *HNPS Advances in Nuclear Physics*, 6, 51–57. <https://doi.org/10.12681/hnps.2915>

Energy Structure and Distribution of Macroscopical Fermion Matter

C.Syros

*Laboratory of Nuclear Technology, University of Patras, 26110 Patras, Greece,
P.O Box 1418*

Abstract

The spatial and energy distribution of fermions are studied in the interior of matter of identical fermions and extremely strong magnetic fields. The vector potential components are $\{A_i = 0, 1, 2, 3\}$ periodic in space. The 4-spinors obey the boundary condition $\Psi = 0$ at finite distance.

1 Introduction

In this paper the discussion of the electromagnetic properties of finitely extended fermion matter [1,2] is continued. The study of the fermion matter under extreme conditions of very high magnetic fields [3] presents particular interest for astrophysics in general as well as in neutron stars and black holes. It is of particular interest also to apply boundary conditions at macroscopically finite distances by far larger than the nuclear scale. This is necessary because real fermion systems obey the Dirac equation independently of their extensions [4].

While the analytic study of the spinors for the description of systems like the presented above is continued [5] here numerical methods are used to find the energy spectrum of the fermions inside extremely strong magnetic fields as well as the current and the density distributions.

The use of the Dirac equation instead of the Schroedinger equation is preferred not only because of the relativistic energies but also for exact description of the spins and the magnetic moments implying strong forces in present situation.

2 The Magnetic and the Nuclear Interactions

The Dirac equation is applied using the vector potential in one space dimension of the form (fig.1)

$$A_k = a_{0k} + a_{k1} \cos(a_k r), \quad k = 1, 2, 3 \quad (1)$$

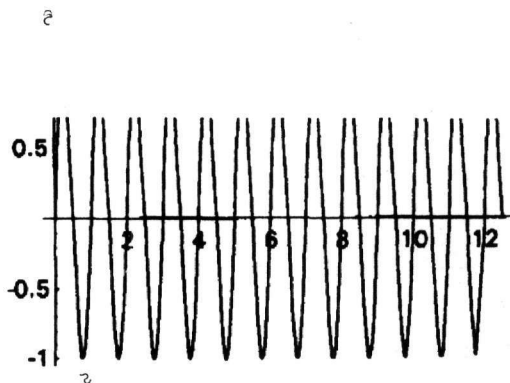


Fig 1. The magnetic field components are periodic functions in space

The values of the constants in the vector potential are as follows:

$$\begin{aligned} a_{00} &= e & a_{20} &= 2e & a_{30} &= 2e \\ a_{11} &= 3/2e & a_{21} &= 5/2e & a_{31} &= 5/2e \end{aligned}$$

where $e = 1.602 \times 10^{-19} \text{C}$ and $a_k = 2\pi$.

With these parameters the magnetic field has the components:

$$\begin{aligned} B_1 &= 0 \quad \text{Tesla} \\ B_2 &= 2.5 \times 10^6 \cdot \pi \cdot \sin[2\pi r] \quad \text{Tesla} \\ B_3 &= 2.5 \times 10^6 \cdot \pi \cdot \sin[2\pi r] \quad \text{Tesla} \end{aligned} \quad (2)$$

The fourth component of $A_4(x)$ in the strong interaction potential given by a sum of periodic potentials modified by a parameter to avoid singularities at the points $r - \lambda = 0$ (fig.2).

$$A_k(r) = g \sum_{\lambda=1}^{\Lambda} \exp[-(|r - \lambda| - s)/r_0] / [|r - \lambda| + s], \quad (3)$$

In (2) $r_0 = 1.2 \times 10^{-15}m$ and s the regularization parameter, $s = 0.5m$, while the interaction constant $g = 3e^2/(10 \times \epsilon_0 r_0)$, and $\epsilon_0 = 8.854 \times 10^{-12}$ MKSA.

The integer Λ gives the number of the one-fermion layers in the fermion matter bulk.

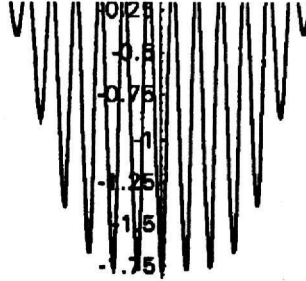


Fig 2. Strong interaction potential of 17 fermions inside extended fermion matter

3 The Dirac equation

In order to solve the Dirac equation

$$\sum_{\mu}^{\Lambda} \gamma_{\mu} D_{\mu} \Psi + k \Psi = 0 \quad (4)$$

with $D_{\mu} = \partial_{\mu} - \frac{ie}{\hbar c} A_{\mu}$, the strong interaction potential $V = -ieA_4$, for the time independent case

$$\Psi = \Psi e^{-iEt/\hbar} \quad \text{and} \quad \Psi = \begin{bmatrix} y_1 \\ y_2 \\ y_3 \\ y_4 \end{bmatrix} \quad (5)$$

with macroscopic boundary conditions one has to introduce appropriate normalizations.

Hence, the energies are expressed in units of m_0c^2 , the rest energy of the fermion. The lengths are measured in r_0 units. Under these definitions and using the standard representation for the Dirac matrices ($\gamma_\mu; \mu = 1, 2, 3, 4$) the equation takes on the form

$$\begin{aligned}
 iqy'_1 + a_1y_1 + ia_2y_1 - a_0y_2 + (1 + p + v)y_4 &= 0, \\
 iqy'_2 - a_1y_2 - ia_2y_2 - a_3y_1 + (1 + p - v)y_3 &= 0, \\
 -iqy'_3 - a_1y_3 - ia_2y_3 - a_3y_4 + (1 - p + v)y_2 &= 0, \\
 -iqy'_4 - a_1y_4 + ia_2y_4 - a_3y_3 + (1 + p + v)y_1 &= 0,
 \end{aligned} \tag{6}$$

and $q = \hbar/mc$.

The boundary conditions for obtaining the solutions $\{y_\mu; \mu = 1, 2, 3, 4\}$ of (4) are

$$y_\mu(\Lambda + 1) = 0, \quad \mu = 1, 2, 3, 4 \tag{7}$$

which implies no fermion can leave the matter bulk.

4 Numerical Results

Results have been obtained for situations of various thicknesses of the bulk matter. Also, the investigation has been made with magnetic field and without magnetic field. The strong interaction field has always been of the same form.

The results contain the energy spectrum of the fermion, the density distribution, the three space components of the spinor and the current density (Figs. 3-8).

As expected, the energy eigenvalues are lower in the absence of the magnetic fields.

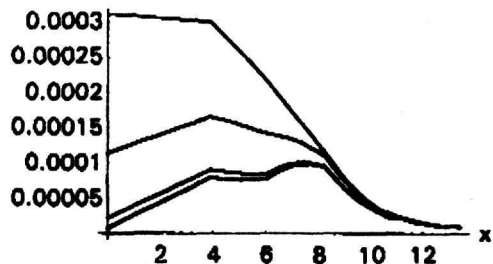


Fig 3. The components of the 4-spinor for a linear system of 24 fermions. Due to symmetry only the rhs half of the graph is shown. The boundary condition is at 12 length units. It is reminded that the heaviest stable nucleus corresponds to about 6 length units.

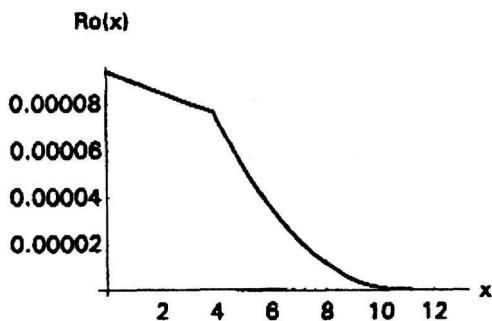


Fig 4. The density distribution of the fermions in the bulk system of the fermion matter. The attraction is stronger towards the central region due to the strong magnetic field.

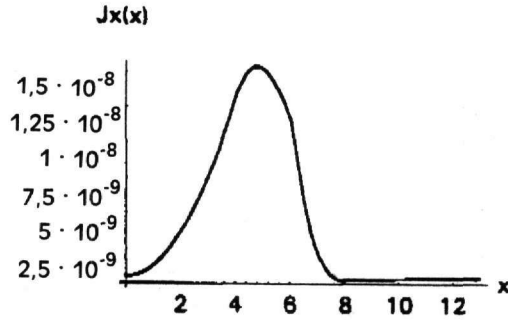


Fig 5. The current density distribution along the x-axis under the influence of the magnetic field.

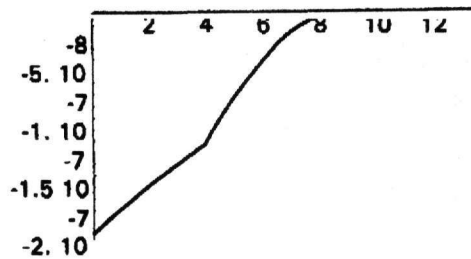


Fig 6. Current density distribution along the y-axis. It is negative as it should due to the continuity equation.

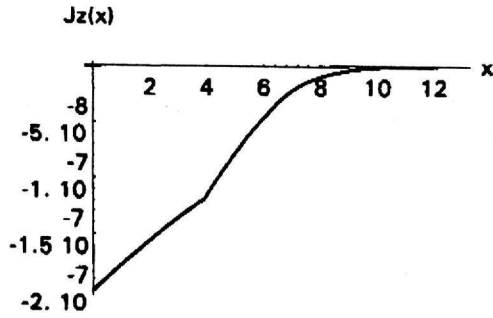


Fig 7.The current density distribution along the z-axis is also negative for conservation reasons of the electric charge.

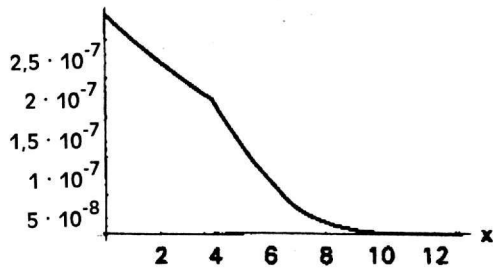


Fig 8.Total density distribution. It vanishes at the boundary of the system so that no electric charge leaves the fermion matter.

References

- [1] A.R.Bodmer, Phys.Rev. D4 (1971) 1601
- [2] E.Witten, Phys.Rev. D30(1984) 272
- [3] E.Fahri and R.L.Jaffe, Phys.Rev. D30 (1984) 2379
- [4] C.Syros, (Vrhndlg. of DPG, Mainz, 1993/4, ISSN 0420-0195) p.638
- [5] A.Kechriniotis and C.Syros, Proc. 5th Symp. Of Nuclear Physics Patras, 6-7 May 1994, European Commission, EUR 16302 EN, p.223-241.